[CANCER RESEARCH 62, 2220–2226, April 15, 2002]

Advances in Brief

α-Methylacyl-CoA Racemase: A New Molecular Marker for Prostate Cancer[1]

Jun Luo, Shan Zha, Wesley R. Gage, Thomas A. Dunn, Jessica L. Hicks, Christina J. Bennett, Charles M. Ewing, Elizabeth A. Platz, Sacha Ferdinandusse, Ronald J. Wanders, Jeffrey M. Trent, William B. Isaacs,[2] and Angelo M. De Marzo

Brady Urological Institute [J. L., S. Z., T. A. D., C. M. E., W. B. I., A. M. D.] and Department of Pathology [W. R. G., J. L. H., C. J. B., A. M. D.], Johns Hopkins University, School of Medicine, Baltimore, Maryland 21287; Department of Epidemiology, Johns Hopkins University, Bloomberg School of Public Health, Baltimore, Maryland 21205 [E. A. P.]; National Human Genome Research Institute, NIH, Bethesda Maryland 20892 [J. M. T.]; and Departments of Pediatrics, Emma Children's Hospital, Clinical Chemistry, Academic Medical Centre, University of Amsterdam, 1105 AZ Amsterdam, the Netherlands [S. F., R. J. W.]

Abstract

Identification of genes that are dysregulated in association with prostate carcinogenesis can provide disease markers and clues relevant to disease etiology. Of particular interest as candidate markers of disease are those genes that are frequently overexpressed. In this study, we describe a gene, *α-methylacyl-CoA racemase* (AMACR), whose expression is consistently up-regulated in prostate cancer. Analysis of mRNA levels of AMACR revealed an average up-regulation of ~9 fold in clinical prostate cancer specimens compared with normal. Western blot and immunohistochemical analysis confirms the up-regulation at the protein level and localizes the enzyme predominantly to the peroxisomal compartment of prostate cancer cells. A detailed immunohistochemical analysis of samples from 168 primary prostate cancer cases using both standard slides and tissue microarrays demonstrates that both prostate carcinomas and the presumed precursor lesion (high-grade prostatic intraepithelial neoplasia) consistently scored significantly higher than matched normal prostate epithelium; 88% of the carcinomas had a staining score higher than the highest score observed for any sample of normal prostate epithelium. Both untreated metastases ($n = 32$ patients) and hormone refractory prostate cancers ($n = 14$ patients) were generally strongly positive for AMACR. To extend the utility of this marker for prostate cancer diagnosis, we combined staining for cytoplasmic AMACR with staining for the nuclear protein, p63, a basal cell marker in the prostate that is absent in prostate cancer. In a simple assay that can be useful for the diagnosis of prostate cancer on both biopsy and surgical specimens, combined staining for p63 and AMACR resulted in a staining pattern that greatly facilitated the identification of malignant prostate cells. The enzyme encoded by the *AMACR* gene plays a critical role in peroxisomal β oxidation of branched chain fatty acid molecules. These observations could have important epidemiological and preventive implications for prostate cancer, as the main sources of branched chain fatty acids are dairy products and beef, the consumption of which has been associated with an increased risk for prostate cancer in multiple studies. On the basis of its consistency and magnitude of cancer cell-specific expression, we propose AMACR as an important new marker of prostate cancer and that its use in combination with p63 staining will form the basis for an improved staining method for the identification of prostate carcinomas. Furthermore, the absence of AMACR staining in the vast majority of normal tissues coupled with its enzymatic activity makes AMACR the ideal candidate for development of molecular probes for the noninvasive identification of prostate cancer by imaging modalities.

Introduction

Prostate cancer initiation and progression are processes involving multiple molecular alterations (1). Genomic alterations, combined with changes in the tissue microenvironment, lead inevitably to altered levels of expression of many individual genes in tumor cells. Identification of these genes represents a critical step toward a thorough understanding of prostate carcinogenesis and an improved management of prostate cancer patients. Of particular biological and clinical interest are those genes that are consistently overexpressed in the vast majority of prostate cancers. Such genes and their products, besides providing possibly valuable insight into the etiology of prostate cancer, may have important utility as diagnostic markers in this disease. However, few genes of this nature have been reported to date.

High-throughput gene expression profiling using cDNA microarray allows for systematic interrogation of transcriptionally altered genes. By comparing the mRNA expression profile of cancerous lesions with noncancerous lesions, multiple candidates of molecular markers for prostate cancer have emerged (2–6). One such candidate, the gene for AMACR,[3] was identified as being overexpressed in prostate carcinoma cells when compared with benign or normal prostate epithelial cells (2, 3). AMACR is a well-characterized enzyme (7) that plays a key role in peroxisomal β-oxidation of dietary branched-chain fatty acids and C27-bile acid intermediates. It catalyzes the conversion of (R)-α-methyl-branched-chain fatty acyl-CoA esters to their (S)-stereoisomers. Only the (S)-stereoisomers can serve as substrates for branched-chain acyl-CoA oxidase during their subsequent peroxisomal β-oxidation. Two aspects of this pathway may have particular relevance for prostate carcinogenesis: (*a*) the main sources of branched chain fatty acids in humans (milk, beef, and dairy products; Ref. 8) have been implicated as dietary risk factors for prostate cancer (9); and (*b*) peroxisomal β-oxidation generates hydrogen peroxide (10), a potential source of procarcinogenic oxidative damage (11, 12).

An initial report by Xu *et al.* (2), using a limited number of samples, indicated that AMACR was overexpressed potentially in a subset of prostate cancers at both the mRNA and protein level. Our previous study compared gene expression profiles of 16 prostate cancer and 9 samples of BPH using cDNA microarrays containing 6500 human genes (3). AMACR was expressed highly in the majority of prostate cancer samples, averaging ~6-fold higher levels than the BPH samples. In this study, we expanded these previous studies by including cDNA microarray data from an additional 35 prostate tissue samples, comprising matched normal tumor pairs, and by performing an extensive IHC analysis of both primary and metastatic prostate cancer specimens, including normal and cancerous prostate tissue from 159 patients analyzed on prostate TMAs. Furthermore, we examined the diagnostic utility of combining staining for AMACR with staining for p63, a prostate basal cell marker that is absent in the vast majority of prostate cancers (13, 14). The consistent and extensive up-regulation

Received 11/19/01; accepted 3/4/02.

The costs of publication of this article were defrayed in part by the payment of page charges. This article must therefore be hereby marked *advertisement* in accordance with 18 U.S.C. Section 1734 solely to indicate this fact.

[1] Supported by the Peter Jay Sharp Foundation and PHS Grants CA58236 and CA78588 and a grant from the Charlotte Geyer Foundation.

[2] To whom requests for reprints should be addressed, at Marburg 115, Johns Hopkins Hospital, 600 North Wolfe Street, Baltimore, MD 21287.

[3] The abbreviations used are: AMACR, α-methylacyl-CoA racemase; IHC, immunohistochemical; KRT8, keratin 8; PIN, prostatic intraepithelial neoplasia; TMA, tissue microarray; BPH, benign prostatic hyperplasia; TBP, TATA-binding protein; GSTP1, glutathione *S*-transferase π; HGPIN, high-grade prostatic intraepithelial neoplasia.

of AMACR that we observe at both the mRNA and protein level strongly suggests that AMACR will be an important new marker for prostate cancer.

Materials and Methods

Prostate Tissue Procurement for cDNA Microarray Analysis. Prostate cancer tissue specimens for cDNA microarray analysis were obtained from 23 patients undergoing radical prostatectomy for clinically localized prostate carcinoma at Johns Hopkins Hospital from 1993 to 2000. Specimens were obtained from the operating room immediately after resection. The seminal vesicles were truncated. If palpable tumor was identified, the specimen was inked and harvested as described previously (15). This results in the banking of the largest palpable tumor, as well as areas of apparent normal and BPH when available. The areas containing tumor that were adjacent to the harvested tumor blocks were submitted for formalin fixation and routine processing. Harvested tissues were flash frozen and stored in −80°C. Paired normal cancer samples were prepared as described previously (3) from 12 of the 23 specimens, whereas only cancer samples were obtained from the other 11 specimens, giving 35 samples total for analysis. Cancer samples were microscopically estimated to contain ≥60% (range from 60 to 90%) adenocarcinoma cells in cellular composition, and the normal samples were estimated to contain ≥50% (range from 50 to 75%) epithelial cells. Institutional Review Board-approved informed consent was obtained from all patients in this study.

cDNA Microarray Analysis. RNA extraction, labeling, and hybridization were carried out as described previously (3). A single reference sample composed of a pool of RNA from two BPH specimens was used throughout all hybridizations. Measurement values were extracted for normalized ratios of signal intensities of sample *versus* reference, which represent the relative mRNA abundance for each gene in each sample when compared with the common reference (3).

Real-time Reverse Transcription-PCR. Quantitative PCR was performed on iCycler (Bio-Rad, Richmond, CA) with gene-specific primers (AMACR: 5′-GAATCCGTATGCCCCGCTGAATCT-3′ and 5′-ACCCTTGCCAGTGCGTGTGC-3′; TBP: 5′-CACGAACCACGGCACTGATT-3′ and 5′-TTTTCTTGCTGCCAGTCTGGAC-3′), as described previously (16). A standard curve was generated by serial dilution of plasmids containing the specific amplicons assayed. AMACR mRNA copy number was normalized to TBP.

Western Blot Analysis. Protein (25 μg) was subjected to SDS–polyacrylamide (10%) gel electrophoresis, transferred to nitrocellulose (Amersham Pharmacia Biotech, Piscataway, NJ), probed with AMACR antiserum (7) at a 1:2000 dilution, and detected by enhanced chemiluminescence (Amersham Pharmacia Biotech) as described previously (16).

TMAs: Construction and Analysis. A total of 159 radical prostatectomy specimens were selected randomly out of a total of >400 cases performed between 1/1/2000 and 8/1/2001 at Johns Hopkins Hospital and used to construct TMAs as described previously (16). Areas representing the largest carcinoma present, as well as areas of normal appearing prostate epithelium, were circled on the glass slides. For each sample of tumor and normal, four tissue cores were taken for TMA construction. Although there is no universal method of sampling prostate cancer tissue for IHC studies, using either standard slides or TMAs, the histological features of these areas that we sampled generally reflect the final Gleason score for the case. Stained TMA slides were scanned using the BLISS imaging system as described by Manley *et al.* (17). Each array spot was then formed into a composite image and viewed and scored on a personal computer monitor as described (16). Data were then further summarized, and statistical analysis was performed using Stata 6.0 and SAS for Microsoft Windows.

Prostate Adenocarcinoma Tissue from Standard Slides. For a number of the cases, standard slides were used to assess overall percentage of positive cells in the tumors and normal tissues and also to further evaluate expression in HGPIN and BPH.

Metastatic Prostate Cancers. For metastatic carcinoma, standard slides from specimens (pelvic lymph node, soft tissue, and bone metastases) from patients with nonhormone refractory tumors were obtained from the archives of the Department of Pathology at The Johns Hopkins University. For hormone refractory cancer specimens, tissues were obtained as a single TMA from the University of Michigan, Specialized Programs of Research Excellence core tissue facility.

IHC Staining. Staining for AMACR was carried out using the Envision+ kit (DAKO Corp., Carpinteria, CA). Briefly deparaffinized slides were hydrated and then placed in citrate buffer (pH 6.0) and steamed for 14 min. Endogenous peroxidase activity was quenched by incubation with DAKO peroxidase block for 5 min at room temperature. Slides were then washed and incubated with primary antibody (1:16,000 dilution of antiserum) overnight at 4°C. Secondary antirabbit antibody-coated polymer peroxidase complex was applied for 30 min at room temperature. Substrate/chromogen was applied and incubated for 5–10 min at room temperature. Slides were counterstained with hematoxylin. For double labeling of AMACR and p63, the anti-p63 mouse monoclonal antibody cocktail (1:100 dilution; Lab Vision Corp., Fremont, CA) was added after the anti-racemese antibody incubation and incubated for 45 min at room temperature. The secondary antirabbit and antimouse HRP conjugates were sequentially added, and the reaction was developed as above.

Scoring of IHC Staining. A scoring method was based on the fact that the specimens clearly showed a varying degree of staining intensity and percentage of cells staining. Therefore, a combined intensity and percentage positive scoring method was used (18). Strong intensity staining was scored as 3, moderate as 2, weak as 1, and negative as 0. For each intensity score, the percentage of cells with that score was estimated visually. A combined weighted score consisting of the sum of the percentage of cells staining at each intensity level was calculated for each sample, *e.g.,* a case with 70% strong staining, 10% moderate staining, and 20% weak staining would receive a score as follows: $(70 \times 3 + 10 \times 2 + 20 \times 1) = 250$. The maximum score is 300.

Results

Analysis of Paired Samples of Normal and Cancerous Prostate Tissue mRNA. In the previous study, we used weighted gene and random permutation analysis to identify 210 genes with statistically different levels of mRNA expression between prostate cancer and BPH (3). Among these genes, AMACR maintained consistently low levels of expression in 9 of 9 BPH samples (signal intensities in the lowest quartile of all genes analyzed) but was overexpressed by an average of 5.7-fold in 13 of 16 cancer samples. We have since generated mRNA profiles of an additional 35 prostate samples, including 12 matched normal cancer pairs and 11 nonpaired cancer samples (data set in preparation for publication) by comparing each sample to a common reference (from BPH). To illustrate the expression pattern of AMACR in these samples in relation to other genes whose expression in prostate tissues has been well documented previously, we extracted expression ratios for AMACR (IMAGE clone ID: 133130), along with those for GSTP1 (IMAGE clone ID: 136235) and KRT8 (IMAGE clone ID: 897781). Reduced GSTP1 expression because of "CpG island" hypermethylation is found in >90% of prostate cancers (19), and KRT8 mRNA is expressed constitutively in the epithelial cells of normal and cancerous prostate tissues (20). As shown in Fig. 1, the majority (20 of 23) of the cancer samples demonstrated overexpression of AMACR mRNA compared with the BPH reference. When the cancer samples were compared with their matching normal samples, AMACR was overexpressed in the cancer samples in 9 of 12 pairs. Moderate overexpression compared with the reference (an average of 3-fold) was also observed in 3 of the 12 normal samples. Consistent with previous reports, GSTP1 expression was down-regulated in the majority of cancer samples compared with BPH reference or their matching normal samples. Expression of KRT8, an epithelial marker, showed little variation among all of the samples, indicating that the sample preparation was effective to enrich and balance the epithelial content in the samples analyzed.

A quantitative reverse transcription-PCR assay was used to estimate the relative difference in AMACR mRNA abundance in samples of normal and cancerous prostate tissue. Although extensive variability was observed, the copy number of AMACR mRNA in prostate cancer specimens was on average 8.8-fold higher than the value for normal prostate samples (average = 60.9, SD = 84.3, range 0.6–260.4, n = 8, for cancer samples compared with an average of 6.9,

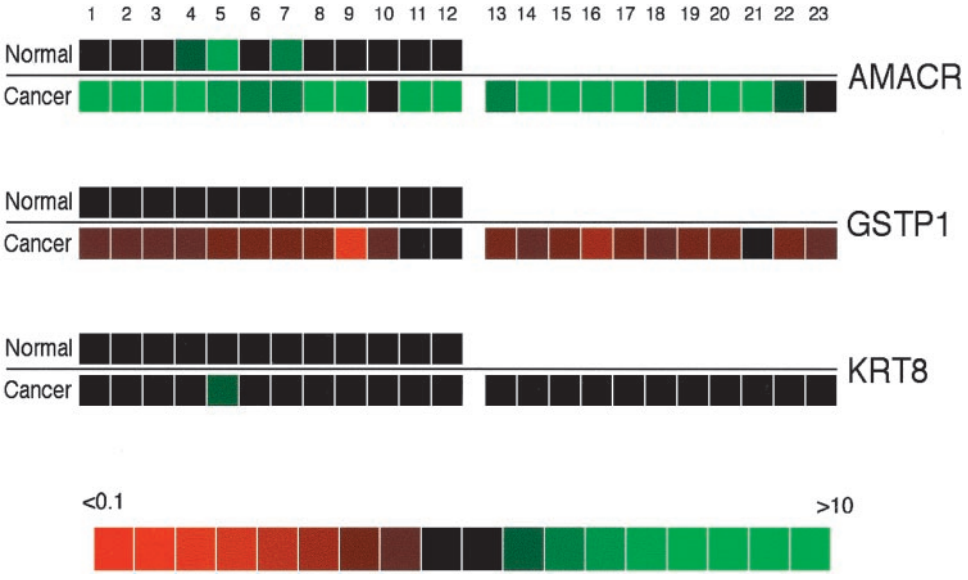

Fig. 1 Gene expression ratios for AMACR, GSTP1, and KRT8. Each *colored square* represents the relative mRNA abundance (ratio of sample: reference) in each sample compared with the common BPH reference. Each of the 12 normal samples (*1–12*) was paired with its matching cancer sample below the *black line* and the other 11 nonpaired cancer samples (*13–23*) positioned at the *right side below* the *line*. The measured expression ratios for each gene were presented graphically as *colored squares*, with the *green squares* representing higher expression in sample compared with the reference (BPH), the *red squares* meaning lower expression in sample than reference (BPH), and *black squares* indicating a ratio of ~1. Color intensities are scaled according to the ratio (sample:reference) as shown at the *bottom*, with the brightest color having a ratio of >10 (*green*) or <0.1 (*red*).

SD = 9.9, range 0.51–32.9, n = 8, for normal) when normalized against copies of TBP. Similarly, the median value for the cancer samples was 7.8-fold higher than for the normal samples.

Western Blot Analysis of AMACR Protein. Expression of AMACR protein was examined using an antiserum demonstrated previously to be specific for this antigen (7). Western blot detection of AMACR in liver, as a positive control (7), and a series of prostate tissue samples is shown in Fig. 2. Although a M_r 47,000 band corresponding to AMACR protein was readily detected in liver and each of the prostate cancer specimens, little or no reactivity was observed in the corresponding normal specimens or any of the BPH samples assayed.

IHC Analysis of Radical Prostatectomy Specimens Using Standard Slides. To obtain the pattern of staining of AMACR in prostate tissues, we examined clinically localized prostate adenocarcinoma specimens using representative standard slides containing normal epithelium, carcinoma, and HGPIN. We used a scoring method that accounts for both the intensity of staining and the percentage of cells staining. In general, normal prostate epithelium was either negative or weakly positive (n = 14 areas from 12 patients, median score = 15, mean score = 19, SD = 22; Fig. 3). Prostate stroma, inflammatory cells, endothelial cells, and nerves were uniformly negative (Fig. 3). Strikingly, adenocarcinomas showed highly intense staining in the majority of tumor cells in most cases (n = 19 carcinoma lesions from 14 patients, median = 290, mean = 277, SD = 30; Fig. 3). The staining was uniformly cytoplasmic and was typically found in small punctate, microbody structures, consistent with the previously reported localization of AMACR predominantly to peroxisomes and mitochondria (7). Staining in HGPIN was also generally positive, although the staining was more variable and often less intense than adjacent carcinoma (Fig. 3, *C* and *D*; n = 10 areas from 6 patients, median 170, mean 179, SD = 63). Staining in atrophic areas was generally negative or positive in a small percentage of cells (n = 5 areas from 3 patients, median = 30, mean = 30, SD = 22). Staining in BPH was generally negative or focally, weakly positive (n = 6 areas from 4 patients, median = 20, mean = 20, SD = 8.9).

IHC Analysis of Radical Prostatectomy Specimens Using TMAs. To survey many tumor and normal specimens, four high-density TMAs, designed to contain samples of clinically localized prostate cancer and matched normal appearing epithelium from 159 patients, were stained. The median age of patients in these TMAs was 58 (range 40–73), and the median prostate-specific antigen was 6.4 (mean 7.5, SD 4.6, range 1.2–38). Array spots (1578) were imaged. The majority of array spots (79%) contained tissue that was readily readable. Of the usable array spot images, 209 were control normal (nonprostatic) tissues. Of the array spots scored for AMACR staining, 417 spots contained adenocarcinoma (334 Gleason pattern 3, 62 Gleason pattern 4, 15 Gleason pattern 5, 4 Gleason pattern 2, 1 ductal adenocarcinoma, 1 pseudo-hyperplastic carcinoma) from 142 patients, 442 spots contained normal prostate epithelium from 144 patients of the patients, and 27 spots contained HGPIN from 23 patients. Other spots consisted of prostate stroma only, atrophy, or were difficult to interpret.

For normal prostate and adenocarcinoma, between 2.5 and 3 TMA spots (duplicate spots) were scored from each patient. For statistical analyses, the mean of the individual spot scores were computed so that for each tissue type from each patient, there was a single IHC score for comparison. Using these mean scores, the AMACR IHC scores for both carcinoma and HGPIN were highly statistically significantly different from normal (Fig. 4, carcinoma *versus* normal, $P < 0.0001$;

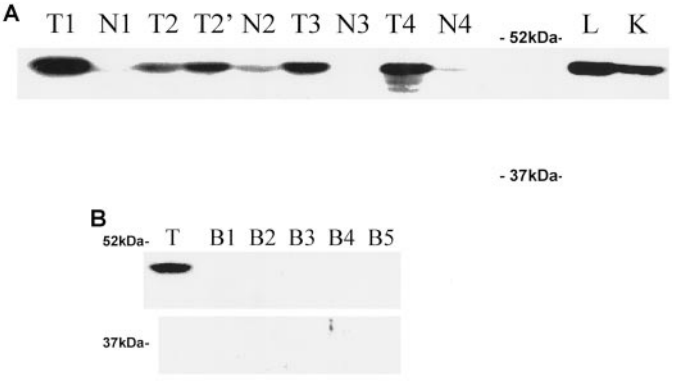

Fig. 2. Western blot analysis of AMACR protein. Total tissue protein (25 μg) was analyzed using anti-AMACR antiserum. In *A*, pairs of tumor and corresponding normal tissue from 4 patients are designated by *T1*, *T2*, *T3*, *T4*, and *N1*, *N2*, *N3*, *N4*, respectively. For the second patient, there were two apparently independent tumors sampled (*T2* and *T2′*). *L*, liver and *K*, kidney. In *B*, five different samples of BPH tissue (*B1–B5*) were analyzed together with a single sample of prostate cancer (*T*). The position of prestained molecular weight markers (ovalbumin at M_r 52,000 and carbonic anhydrase at M_r 37,000) is marked.

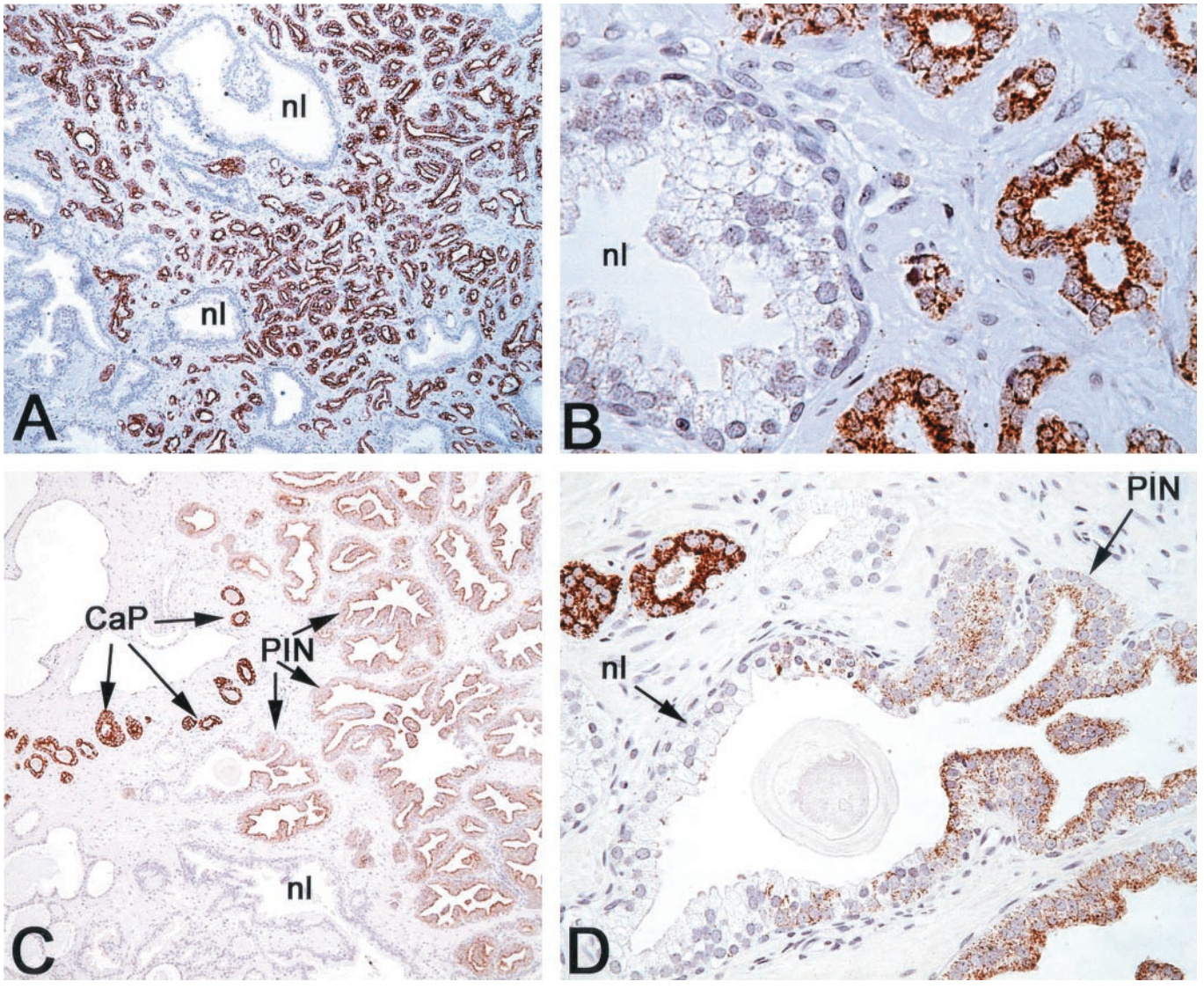

Fig. 3. IHC localization of AMACR in prostate tissue using standard slides. *A*, low-power image of Gleason pattern 3 carcinoma infiltrating between benign normal appearing glands (*nl*) showing homogeneous strong staining (×40). *B*, higher power view of representative region from *A* showing punctate cytoplasmic staining (×400). *C*, another case showing high-intensity staining in carcinoma (*CaP*), intermediate intensity staining in HGPIN (*PIN*), and no staining in normal (*nl*; ×100). *D*, higher power view of *C* showing strong staining in carcinoma glands (*top left*) and staining in acinus in that is involved partially with HGPIN with staining only in atypical HGPIN cells (*PIN*). Note negative staining in the normal appearing acinus just to the *right* of the carcinoma (×200).

HGPIN *versus* normal, $P < 0.001$, Wilcoxon's rank-sum test). The score for HGPIN was significantly less than the score for carcinoma ($P = 0.0002$, Wilcoxon's rank-sum test). If a cutoff of ≥100 is used for positive staining, then 95.6% of carcinomas were positive, whereas 3.5% (5 of 144) of normal epithelium was positive. Using a score of ≥150 for strong positive staining, then 88% of the carcinomas would be considered strong, *versus* none of the normal epithelium. The carcinomas (52%) had a median score of 300 (the maximum).

The distribution of AMACR mean IHC scores for carcinoma (mean for all of the spots for each patient) stratified by Gleason score and pathological stage is shown in Table 1. There was no relation between AMACR IHC score and Gleason grade, pathological stage, patient age, or preoperative serum prostate-specific antigen (Kruskal-Wallis, all *P*s > 0.05). As expected, Gleason score at radical prostatectomy was associated strongly with higher stage disease (Spearman's rank correlation coefficient = 0.42, $n = 142$, $P < 0.0001$; Table 1).

IHC Analysis of Prostate Cancer Metastases. Staining in metastatic prostate cancers from nonhormone refractory disease ($n = 32$ sites from 32 patients: 8 bone, 21 pelvic lymph node, 2 soft tissue, and 1 lung) showed staining in the majority of cases (data not shown). The median score in nontreated metastatic cases was 240 (mean 204, SD 97). By the criteria stated above for positivity, 81% (26 of 32) were positive, and 62.5% were strongly positive (20 of 32). In hormone refractory metastatic prostate ($n = 25$ sites from 14 patients), the median score was 215 (mean = 206, SD = 84). Thus, 93% (13 of 14) of hormone refractory metastatic cancers were positive, and 71.4% were strongly positive.

AMACR Protein Expression in Other Normal Tissues. To examine the overall tissue distribution of AMACR protein expression, staining was performed using a TMA containing a wide variety of human tissues. Staining was strongly positive in virtually all hepatocytes, proximal kidney tubules, and glomerular epithelial cells of the kidney (data not shown). Moderate staining was found in the acinar cells and some ductal cells of major salivary glands. Weak staining was found in distal tubules and collecting ducts of the kidney. Other tissues showed weak and heterogeneous expression, including the following: (*a*) neurons in the central nervous system; (*b*) absorptive

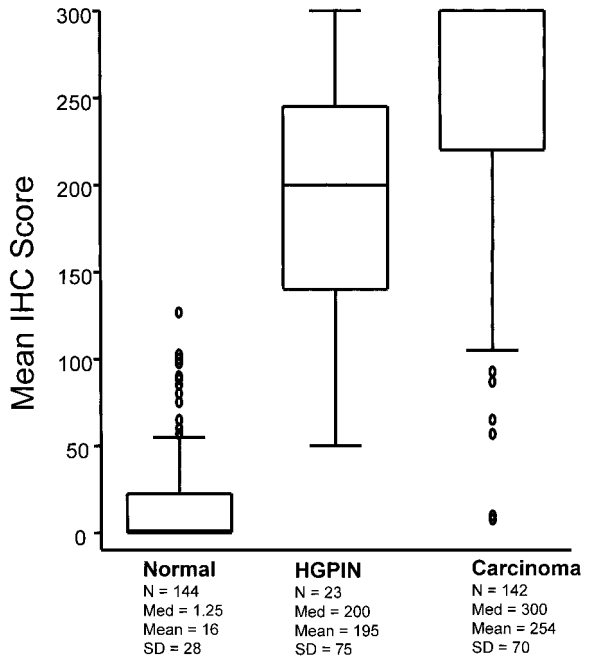

Fig. 4. Relative expression of AMACR by IHC score in normal, HGPIN, and carcinoma by scoring of TMA spots. *Box* shows 25th-75th percentiles, as well as median (*center line*). *Whiskers* show 5th and 95th percentiles, and *ovals* represent outliers.

and paneth cells of the small bowel; (*c*) absorptive cells of the large bowel; and (*d*) Sertoli cells of the testis. Staining was not detectable in the urinary bladder, ovary, endometrium, fallopian tube, uterine cervix, breast, lung, skin, tonsil, lymph nodes, thymus, spleen, laryngeal epithelium, minor salivary glands, pancreas, gall bladder, thyroid, stomach, esophagus, skeletal muscle, or smooth muscle.

Combination of AMACR Staining with p63 Facilitates Detection of Prostate Cancer Cells. The intense staining in tumors with weak staining in normal suggested that AMACR IHC staining might be useful as an adjunct to the diagnosis of prostate cancer on needle biopsy or other clinical specimens. To be useful as a potential diagnostic marker for prostate cancer, carcinoma lesions need to be separated reliably from lesions of HGPIN and other potential mimicars of prostate cancer, such as adenosis and atrophy, as well as from normal prostate tissue. On small needle biopsy samples, this distinction can sometimes be problematic (21). One very useful tool has been IHC staining for basal cell-specific cytokeratins, typically using the 34BE12 monoclonal antibody (22). Because basal cells, which are absent in the vast majority of prostatic adenocarcinomas, are present in normal glands, benign mimicars, such as atrophy and adenosis, and in HGPIN, staining for basal cell cytokeratins is often used in prostate cancer needle biopsies (22). More recently, the p63 protein has been found to be localized to the nuclei of basal cells in prostate epithelium with a basal cell-specific staining pattern nearly identical to 34BE12 (13, 14). Because the staining for p63 is strictly nuclear and is negative in the vast majority of carcinomas, and the staining for AMCAR is cytoplasmic and only strong in carcinoma or HGPIN, we combined the staining for these two markers as a cocktail. There was strong staining of the nuclei of basal cells in benign glands, whereas carcinoma showed no nuclear staining but strong cytoplasmic staining, with no decrease as compared with AMCAR staining alone ($n = 20$, Fig. 5, *A* and *B*). HGPIN showed variable punctate, cytoplasmic AMCAR staining, but strong and homogeneous nuclear staining in basal cells, thus allowing one to reliably distinguish HGPIN from carcinoma (Fig. 5, *C* and *D*). At times, HGPIN appeared to contain buds of epithelium, pinching off into the underlying stroma (23). An example of this phenomenon is shown in Fig. 5*D* (*arrow*), where a single acinus is projecting from an acinus containing HGPIN. The projecting acinus shows very sparse p63 basal cell staining, consistent with early invasion. The surrounding carcinoma cells show complete loss of p63 staining, yet they contain AMACR cytoplasmic staining.

Discussion

In this study, we demonstrate that AMACR is overexpressed in the majority of prostate cancers and cancer cells within these tumors. Using many cases with diverse pathologic characteristics, we find that overexpression at the protein level is very tightly linked to prostate cancer and occurs in virtually all grades and stages and in both hormone refractory and untreated cases. Over 95% of prostate cancers analyzed stained positively for AMACR, whereas <4% of histologically normal prostate epithelium was positive. Using a more stringent scoring scheme, these values are 88 and 0% for cancers and normal cells that are positive, respectively. Because there appears to be such a tight link between overexpression and the histological prostate cancer phenotype, these finding have implications for the pathogenesis, diagnosis, imaging, and treatment of prostate cancer.

In terms of early diagnosis on prostate needle biopsy, whereas basal cell-specific keratin is a useful aid for diagnosis, this marker is lost in prostate cancer. Because there can be artifactual loss of IHC staining, at times, this staining is uninformative and/or misleading. To date, few, if any, validated markers of prostate cancer have been identified that are overexpressed consistently as detected by IHC staining such that they might be of diagnostic use in a large percentage of cases. We now show that AMACR may provide the first example of such a marker. Because AMACR staining can occur intensely in HGPIN, we combined staining using AMACR with staining for p63. Because these markers, when present, are invariably cytoplasmic and nuclear, respectively, there is no need for the use of two color staining. p63 staining has been shown to be comparable with the basal cell-specific keratin 34βE12 monoclonal antibody but has the advantage in this case of a more clearly discernible nuclear location (13, 14). Thus, AMACR is a new positive stain that complements the traditional negative stain to enhance prostate cancer diagnosis. To determine the usefulness of AMACR in diagnostic pathology practice, we have begun to use clinical needle biopsies in prospective studies comparing AMACR, AMACR/p63, and basal cell-specific cytokeratins. Additionally, this marker combination could be of use for nonpathologist researchers studying prostate cancer specimens to enhance diagnostic certainty.

The enzyme encoded by this gene plays a critical role in the metabolism of fatty acid molecules, specifically by peroxisomal β

Table 1 *AMACR IHC score from TMA analysis for 142 patients stratified by Gleason grade and pathological stage at radical prostatectomy*

		Stage			
Grade		T2	T3A	T3B	N1
5–6	n	65	12	2	0
	Median	300	268	258	Na[a]
	Mean	255	218	258	Na
	SD	68	100	60	Na
7	n	24	14	5	1
	Median	293	300	243	300
	Mean	238	263	254	300
	SD	83	60	43	0
8–9	n	5	10	3	1
	Median	300	300	283	300
	Mean	297	274	273	300
	SD	8	58	34	0

[a] Na, not applicable.

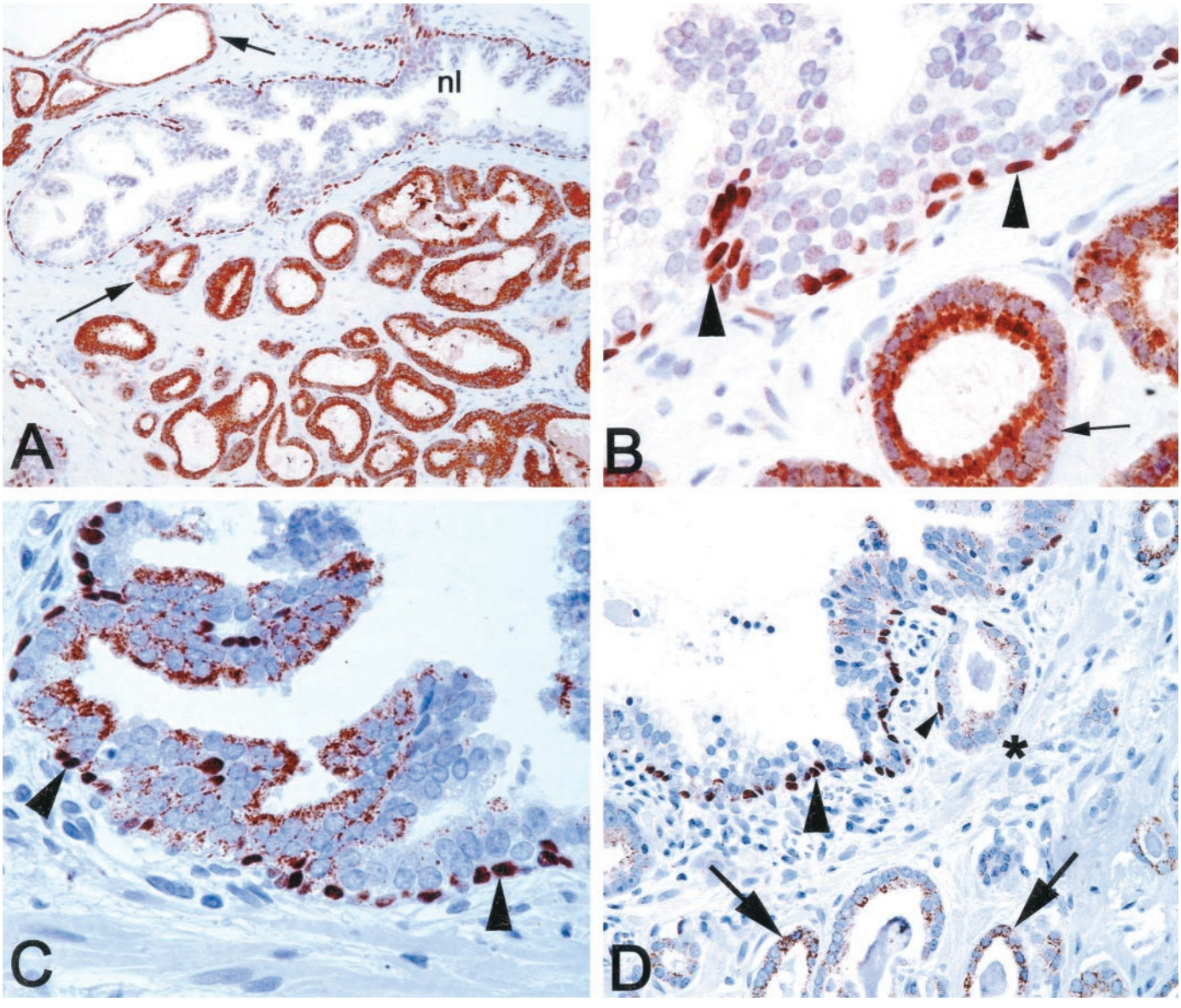

Fig. 5. Simultaneous single color localization of p63 and AMACR. Tissues were stained with a cocktail containing anti-p63 (nuclear) and anti-AMACR (punctate cytoplasmic) antibodies, and staining was localized simultaneously. In *A*, nuclear basal cell staining (p63) is apparent in normal appearing acinus. *Arrows*, infiltrating carcinoma cells (×100). *B*, higher power view of *A*. *Arrowheads*, nuclear basal cells staining (p63); *arrow*, carcinoma (×400). *C*, HGPIN showing moderate to weak punctate cytoplasmic AMACR staining and strong positive staining p63 staining of basal cells (×400). *D*, HGPIN (top gland) with weak cytoplasmic AMACR staining and nuclear basal cells staining (p63). Note small acinus apparently budding off (*) of HGPIN gland showing very sparse basal cell nuclear staining (*arrowhead*). *Below*, there is moderate to weak intensity cytoplasmic staining in infiltrating carcinoma cells that lack p63 nuclear staining.

oxidation (10). Branched chain fatty acids, which originate almost entirely from the diet, contain methyl groups in the R position, whereas the enzymes of the β oxidation pathway can only transform substrates having the S configuration (10). The enzyme AMACR catalyzes this interconversion. One implication of the up-regulation of AMACR is that prostate cancer cells may have a consistently greater capacity to metabolize dietary branched chain fatty acids than would their normal counterparts. Although the contribution of this up-regulation to prostate carcinogenesis, if any, is unclear at present, two interesting aspects of this pathway may be relevant: (*a*) the first step of the pathway in β oxidation of branched chain fatty acids is an oxidation step catalyzed by acyl-CoA oxidases, with the products being oxidized substrate and hydrogen peroxide (10). Experimental overexpression of acyl-CoA oxidase can transform cells (12), and the increase in oxidative stress because of the production of hydrogen peroxide by this pathway has been proposed to play a role in the transformation process (11). Indeed, the potent carcinogenic activity of peroxisome proliferators in animal models is thought to be mediated, at least in part, by up-regulation of the peroxide-producing enzymes of the peroxisome (24); and (*b*) the primary branched chain fatty acid whose metabolism is critically dependent on the action of AMACR is phytanic acid, derived from phytol, a breakdown product of chlorophyll in ruminants. This fatty acid is found primarily in cow's milk, and diary products derived there from, as well as beef but not meat from chickens or some fish (25). An interesting question is whether the increased risk for prostate cancer conferred by consumption of dairy products and/or red meat (9) is related to the up-regulation of this enzyme and its associated pathway in the early stages of prostate carcinogenesis, *e.g.*, in PIN.

Molecular imaging promises the ability to identify individual cells or groups of cells expressing specific proteins or enzymatic activity in real time in living patients (see Louie *et al.*; Ref. 26) The ability to

image AMACR protein or enzymatic activity would likely provide significant value in localization of primary prostate cancer within the prostate. A first application of this would be to help direct the location of needle biopsy sites in the prostate and possibly to assess the extent of cancer within the prostate. In addition, the ability to image AMACR systemically would provide value for detection of metastatic prostate cancer in organs other than the liver and kidney.

The prostate glands of U.S. men are biopsied >1 million times a year, leading to a positive diagnoses of ~180,000 new prostate cancer cases annually. Estimates of equivocal or ambiguous biopsy evaluations that are suspicious for cancer range from 0.3 to 24% (21), resulting in tens of thousands of repeat biopsies. Clearly, markers, which can assist in the accurate evaluation of prostate needle biopsies, are needed urgently. Because of its consistency and robustness, AMACR appears to fit the criteria for such a marker and as such may become routinely used in the pathological diagnosis of prostate cancer. In addition, the biological function of this marker provides exciting new information regarding the etiology of prostate cancer and provides a novel target for prevention and therapeutics. Whether this marker is pathogenic, a potential drug, or *in vivo* imaging target is subject to ongoing studies.

While our manuscript was in preparation, Jiang *et al.* (27) reported overexpression of AMACR by IHC, using a different antibody, in the majority of primary prostate cancers. Although this report did not examine AMACR expression in other tissues, or combine AMACR staining with p63 or evaluate metastatic prostate cancers, the fact that two separate groups simultaneously observe marked overexpression of this protein in primary prostate cancer is a remarkable finding that bolsters the overall importance of AMACR as a new prostate cancer marker.

Acknowledgments

We thank Helen Fedor and Marsella Southerland for their excellent technical assistance in preparing TMAs, Dennis Faith for help with the Microsoft Access database, and Gerrun E. March for diligence in scanning of TMA slides. We thank Dr. Mark Rubin and the University of Michigan Specialized Programs of Research Excellence TMA facility for the hormone refractory prostate cancer TMA. We also acknowledge the generous support of the Peter J. Sharpe Foundation.

References

1. Isaacs, W. B., and Bova, G. S. Prostate cancer. *In:* B. Vogelstein and K. Kinzler (eds.), The Genetic Basis of Human Cancer, pp. 653–660. New York: McGraw-Hill, 1998.
2. Xu, J., Stolk, J. A., Zhang, X., Silva, S. J., Houghton, R. L., Matsumura, M., Vedvick, T. S., Leslie, K. B., Badaro, R., and Reed, S. G. Identification of differentially expressed genes in human prostate cancer using subtraction and microarray. Cancer Res., *60:* 1677–1682, 2000.
3. Luo, J., Duggan, D. J., Chen, Y., Sauvageot, J., Ewing, C. M., Bittner, M. L., Trent, J. M., and Isaacs, W. B. Human prostate cancer and benign prostatic hyperplasia: molecular dissection by gene expression profiling. Cancer Res., *61:* 4683–4688, 2001.
4. Magee, J. A., Araki, T., Patil, S., Ehrig, T., True, L., Humphrey, P. A., Catalona, W. J., Watson, M. A., and Milbrandt, J. Expression profiling reveals hepsin overexpression in prostate cancer. Cancer Res., *61:* 5692–5696, 2001.
5. Bull, J. H., Ellison, G., Patel, A., Muir, G., Walker, M., Underwood, M., Khan, F., and Paskins, L. Identification of potential diagnostic markers of prostate cancer and prostatic intraepithelial neoplasia using cDNA microarray. Br. J. Cancer, *84:* 1512–1519, 2001.
6. Dhanasekaran, S. M., Barrette, T. R., Ghosh, D., Shah, R., Varambally, S., Kurachi, K., Pienta, K. J., Rubin, M. A., and Chinnaiyan, A. M. Delineation of prognostic biomarkers in prostate cancer. Nature, *412:* 822–826, 2001.
7. Ferdinandusse, S., Denis, S., Ijlst, L., Dacremont, G., Waterham, H. R., and Wanders, R. J. Subcellular localization and physiological role of α-methylacyl-CoA racemase. J. Lipid Res., *41:* 1890–1896, 2000.
8. Wanders, R. J. A., Jacobs, C., and Skjeldal, O. H. Refsum disease. *In:* C. R. Scriver, A. L. Beaudet, W. S. Sly, and D. Valle (eds.), The Metabolic and Molecular Bases of Inherited Disease, pp. 3303–3321. London: McGraw Hill, 2001.
9. Chan, J. M., Stampfer, M. J., Ma, J., Gann, P. H., Gaziano, J. M., and Giovannucci, E. L. Dairy products, calcium, and prostate cancer risk in the Physicians' Health Study. Am. J. Clin. Nutr., *74:* 549–554, 2001.
10. Wanders, R. J., Vreken, P., Ferdinandusse, S., Jansen, G. A., Waterham, H. R., van Roermund, C. W., and Van Grunsven, E. G. Peroxisomal fatty acid α- and β-oxidation in humans: enzymology, peroxisomal metabolite transporters and peroxisomal diseases. Biochem. Soc. Trans., *29:* 250–267, 2001.
11. Ockner R. K., Kaikaus R. M., and Bass N. M. Fatty-acid metabolism and the pathogenesis of hepatocellular carcinoma: review and hypothesis. Hepatology, *18:* 669–676, 1993.
12. Tamatani, T., Hattori, K., Naashiro, K., Hayashi, Y., Wu, S., Klumpp, D., Reddy, J. K., and Oyasu, R. Neoplastic conversion of human urothelial cells *in vitro* by overexpression of H2O2-generating peroxisomal fatty acyl CoA oxidase. Int. J. Oncol., *15:* 743–749, 1999.
13. Signoretti, S., Waltregny, D., Dilks, J., Isaac, B., Lin, D., Garraway, L., Yang, A., Montironi, R., McKeon, F., and Loda, M. p63 is a prostate basal cell marker and is required for prostate development. Am. J. Pathol., *157:* 1769–1775, 2000.
14. Parsons, J. K., Gage, W. R., Nelson, W. G., and De Marzo, A. M. Expression of p63 in normal, neoplastic and preneoplastic human prostate tissues. Urology, *58:* 619–624, 2001.
15. Bova, G. S., Fox, W. M., and Epstein, J. I. Methods of radical prostatectomy specimen processing: a novel technique for harvesting fresh prostate cancer tissue and review of processing techniques. Mod. Pathol., *6:* 201–207, 1993.
16. Zha S., Gage W. R., Sauvageot, J., Saria, E. A., Putzi, M. J., Ewing, C. M., Faith, D. A., Nelson, W. G., De Marzo, A. M., and Isaacs, W. B. Cyclooxygenase-2 is up-regulated in proliferative inflammatory atrophy of the prostate, but not in prostate carcinoma. Cancer Res., *61:* 8617–8623, 2001.
17. Manley, S., Mucci, N. R., De Marzo, A. M., and Rubin, M. A. Relational database structure to manage high-density tissue microarray data and images for pathology studies focusing on clinical outcome: the prostate specialized program of research excellence model. Am. J. Pathol., *159:* 837–843, 2001.
18. De Marzo, A. M., Knudsen, B., Chan-Tack, K., and Epstein, J. I. E-cadherin expression as a marker of tumor aggressiveness in routinely processed radical prostatectomy specimens. Urology, *53:* 707–713, 1999.
19. Lee, W. H., Morton, R. A., Epstein, J. I., Brooks, J. D., Campbell, P. A., Bova, G. S., Hsieh, W. S., Isaacs, W. B., and Nelson, W. G. Cytidine methylation of regulatory sequences near the pi-class glutathione *S-transferase* gene accompanies human prostatic carcinogenesis. Proc. Natl. Acad. Sci. U S A, *91:* 11733–11737, 1994.
20. Yang, Y., Hao, J., Liu, X., Dalkin, B., and Nagle, R. B. Differential expression of cytokeratin mRNA and protein in normal prostate, prostatic intraepithelial neoplasia, and invasive carcinoma. Am. J. Pathol., *150:* 693–704, 1997.
21. Epstein, J. I., and Potter, S. R. The pathological interpretation and significance of prostate needle biopsy findings: implications and current controversies. J. Urol., *166:* 402–410, 2001.
22. Wojno, K. J., and Epstein, J. I. The utility of basal cell-specific anti-cytokeratin antibody (34 β E12) in the diagnosis of prostate cancer. A review of 228 cases. Am. J. Surg. Pathol., *19:* 251–260, 1995.
23. McNeal, J. E., Villers, A., Redwine, E. A., Freiha, F. S., and Stamey, T. A. Microcarcinoma in the prostate: its association with duct-acinar dysplasia. Hum. Pathol., *22:* 644–652, 1991.
24. Yeldandi, A. V., Rao, M. S., and Reddy, J. K. Hydrogen peroxide generation in peroxisome proliferator-induced oncogenesis. Mutat. Res., *448:* 159–177, 2000.
25. Flanagan, V. P., Ferretti, A., Schwartz, D. P., and Ruth, J. M. Characterization of two steroidal ketones and two isoprenoid alcohols in dairy products. J. Lipid Res., *16:* 97–101, 1975.
26. Louie, A. Y., Huber, M. M., Ahrens, E. T., Rothbacher, U., Moats, R., Jacobs, R. E., Fraser, S. E., and Meade, T. J. *In vivo* visualization of gene expression using magnetic resonance imaging. Nat. Biotechnol., *18:* 321–325, 2000.
27. Jiang, Z., Woda, B. A., Rock, K. L., Xu, Y., Savas, L., Khan, A., Pihan, G., Cai, F., Babcook, J. S., Rathanaswami, P., Reed, S. G., Xu, J., and Fanger, G. R. P504S: a new molecular marker for the detection of prostate carcinoma. Am. J. Surg. Pathol., *25:* 1397–1404, 2001.